scientific reports

Check for updates

OPEN

A survey of bacterial and fungal community structure and functions in two long-term metalliferous soil habitats

Ashvini Chauhan✉, Christian Chukwujindu, Ashish Pathak & Rajneesh Jaswal

Mercury contamination at legacy nuclear sites such as the Savannah River Site and Oak Ridge Reservation poses persistent ecological risks, yet its impact on soil microbiomes remains incompletely understood. This study integrates qPCR, 16S/ITS amplicon sequencing, and shotgun metagenomics to assess bacterial and fungal community structure, diversity, and functional potential across gradients of total mercury, methylmercury, and bioavailable mercury. Bacterial α-diversity declined with increasing Hg levels, while fungal diversity remained stable and highest in low-contamination soils. Dominant bacterial phyla included Pseudomonadota, Bacteroidota, Bacillota, Acidobacteriota, and Actinomycetota; fungal communities were primarily Ascomycota and Basidiomycota. Canonical correspondence analysis revealed distinct taxon–Hg speciation linkages, and functional gene profiling showed enrichment of stress-response genes, membrane transporters, and phosphate metabolism pathways in contaminated soils. Notably, bioavailable Hg did not correlate directly with total Hg, underscoring the importance of speciation in microbial exposure. These findings highlight the adaptive plasticity of native microbiomes and identify microbial taxa and pathways relevant to bioremediation and can guide ecosystem restoration activities in Hg-impacted soil habitats.

Keywords Mercury, Methylmercury, Bioavailable mercury, Soil microbiome, Metagenomics, Bioremediation, Savannah River site (SRS), Oak ridge reservation (ORR)

Mercury (Hg) is among the top ten chemicals of public-health concern due to its toxicity, persistence, and global distribution[1]. Although naturally occurring, Hg remains widely used in metallurgy, electronics manufacturing, and fluorescent lighting[2]. In the environment, Hg occurs as inorganic Hg(II), elemental Hg(0), and the microbially produced monomethylmercury (MeHg), with speciation governed by local geochemistry and biology[3]. MeHg is particularly hazardous because it is neurotoxic, carcinogenic, and bioaccumulative[4], Hg exposure also threatens organisms across the tree of life, including humans[5]. Once released, Hg is transported and transformed by both natural and anthropogenic processes, including volcanic activity, fossil-fuel combustion, mining, and industrial operations such as chlor-alkali production[6]. Under favorable conditions, microorganisms convert inorganic or elemental Hg to MeHg, which biomagnifies through aquatic food webs[7], contributing to metabolic, renal, neurological, and cardiovascular disorders[8], as also impairing terrestrial and aquatic ecosystems[5].

Microbes are central to Hg cycling and remediation. Mercury-resistant (HgR) bacteria in contaminated environments can volatilize Hg via mer operon–encoded enzymes: *merA* (mercuroreductase) reduces Hg(II) to Hg(0), and *merB* (organomercurial lyase) cleaves C–Hg bonds, enabling detoxification[9,10]. Some bacteria (e.g., *Escherichia*, *Bacillus*, *Streptomyces*) can re-oxidize Hg(0) to Hg(II) via catalase/peroxidase activity[11]. Historically, Hg methylation was attributed mainly to anaerobes, but hgcAB has now been identified across diverse lineages-including iron- and sulfate-reducing bacteria (SRBs), syntrophic Bacillota, and members of Bacteroidota—expanding the known methylator guilds[12]. In Bacillota, species such as *Bacillus*, *Clostridium*, and *Paenibacillus* are well-documented for harboring *merA* and *merB* genes- enzymes that facilitate the reduction of Hg^{2+} to volatile Hg^{0} and the cleavage of methylmercury (MeHg) into less toxic forms. Within Bacteroidota, genera such as *Flavobacterium* and *Sphingobacterium* have shown resistance to mercury and may possess partial detoxification pathways, although the presence of complete mer operons is less common. Conversely, microbial demethylation occurs aerobically and anaerobically, often involving mer-regulated pathways[12].

Microbiomics Laboratory, School of the Environment, Florida A&M University, 1515 S. Martin Luther King Blvd., Suite 305B FSHSRC, Tallahassee, FL 32307, USA. ✉email: ashvini.chauhan@famu.edu

In fact, across Hg-impacted sites, bacterial communities are typically dominated by Pseudomonadota, Bacillota, and Actinomycetota[13,14], with Verrucomicrobiota and Campylobacterota also observed in MeHg-impacted sediments at ORR[15]. Our prior work at the Savannah River Site (SRS) and Oak Ridge Reservation (ORR) combined genomic, proteomic, and physiological approaches to isolate HgR taxa (e.g., *Arthrobacter*, *Serratia*, *Stenotrophomonas*) that harbor *merA*/*merB* and mer regulators[14,16–18]; our findings have also shown that long-term metal exposure may co-select for antibiotic resistance in soils at two former U.S. nuclear legacy sites: SRS (South Carolina) and ORR (Tennessee), respectively.

Despite decades of work on bacterial Hg cycling, fungal mechanisms remain comparatively underexplored. Fungi often tolerate high-Hg conditions[19] as evidenced in strains isolated from wastewater and mining sites (e.g., *Candida*, *Pichia*, *Aspergillus*, *Cladosporium*, *Trichoderma*, *Alternaria*[20–22], employing biosorption, bioaccumulation, and enzymatic transformation mechanisms, potentially via metallothioneins and glutathione-mediated sequestration[21]. Putative fungal contributions to MeHg methylation/demethylation have been proposed, but the underlying genetic bases remain unclear. To this end, to investigate fungal contributions to mercury cycling, we employed diffusion chambers (DC) and microbial traps (MT), which allow in situ-like microbial interactions while enabling nutrient exchange through semipermeable membranes using SRS soils. These methods enriched HgR bacteria (e.g., *Chthoniobacter, Bradyrhizobium, and Burkholderia*) and fungi (e.g., *Penicillium*, *Trichoderma*), potentially involved in Hg methylation or demethylation.

Despite growing interest in microbial responses to mercury (Hg) contamination, several key research gaps remain. First, cross-kingdom integration is limited: bacterial responses to Hg are comparatively well characterized, whereas fungal dynamics remain poorly resolved, and co-variation between bacterial and fungal communities under chronic Hg exposure has been rarely examined. Second, Hg speciation and exposure pathways are often under-modeled; many field studies focus primarily on total Hg (THg), while the more toxic and bioaccumulative methylmercury (MeHg) and bioavailable Hg (BHg), which determine microbial exposure potential, are infrequently analyzed together, weakening mechanistic inference. Third, functional responses are often inferred rather than measured; while amplicon-based predictive pipelines can suggest potential gene functions, shotgun metagenomic approaches that directly quantify gene and metabolic pathway repertoires across Hg gradients remain uncommon. Additionally, long-term, multi-site studies are scarce, with few investigations spanning multiple legacy sites with distinct contamination histories and climatic contexts, limiting the generality of observed patterns. Finally, the temporal stability of microbial responses remains unclear, as the persistence of taxonomic and functional shifts across seasons under chronic Hg stress is not well established. In this study, we address some of the above-stated knowledge gaps by conducting a comprehensive evaluation of bacterial (16S) and fungal (ITS) community assemblages alongside evaluating gene functional shifts across high/medium/low gradients of THg, MeHg, and BHg at the SRS (South Carolina, USA) and ORR (Tennessee, USA) ecosystems.

SRS is a former nuclear weapons production facility with soil and wetland ecosystems that remain co-contaminated with nuclear waste materials, including mercury (Hg), uranium (U), and nickel (Ni)[23]. Similarly, during the mid-twentieth century, nuclear weapons production at the Oak Ridge Y-12 plant released significant amounts of elemental mercury into East Fork Poplar Creek[24]. Despite the cessation of these activities decades ago, mercury concentrations at both sites remain high, ranging from 9.80 ng/g to 1688 ng/g[25]. Therefore, the SRS and ORR ecosystems provide contrasting operational histories where Hg in the soils and sediments remains elevated even decades after the initial release, underscoring the continued need for effective monitoring and remediation efforts[23–25]. To address the long-term impacts of Hg in soils, we performed this integrated study using qPCR, amplicon sequencing (with PICRUSt2 used strictly to support amplicon-based functional inference), and metagenomes to: (i) evaluate bacterial vs. fungal community structure and diversity across variable levels of Hg contamination; (ii) evaluate correlations between dominant bacterial and fungal taxa to Hg speciation via constrained ordination; (iii) test whether stress-response, membrane-transport, and core metabolic pathways are consistently enriched across Hg-contaminated sites and seasons; and (iv) identify taxon–function–environment linkages that highlight resident microbial pathways relevant to Hg resistance and bioremediation at the SRS and ORR former nuclear-legacy sites.

Materials and methods

Site description and sample collection

Soil samples were collected from two former nuclear legacy U.S. Department of Energy (DOE) sites: the Savannah River Site (SRS) near Aiken, South Carolina, and East Fork Poplar Creek (EFPC) within the Oak Ridge Reservation (ORR), Oak Ridge, Tennessee[26]. Both sites have a long history of contamination with heavy metals and organic compounds[24].

From the SRS ecosystem, four samples (SRSS1–SRSS4) were collected from distinct locations in Steed Pond (Tims Branch watershed)- an area impacted by historical heavy-metal inputs[27]. Two additional samples (HO2-1 and HO2-2) were collected from the constructed wetland system treating runoff from the SRS Tritium Processing Facility[28]. A reference/background site (R1/ R2) was selected along SRS Mills Branch, with no known direct soil contaminants beyond regional atmospheric Hg deposition[14]. From the ORR ecosystem, three soils (SoilA, SoilB, and SoilC) were collected from EFPC- these sites represent soil/ sediments with a well-established history of high mercury contamination[24]. Due to the extensive contamination at the ORR site, a suitable reference site could not be located. Triplicate surficial soils were collected, stored on ice, and shipped overnight to the FAMU laboratory for each location. Geographic coordinates for all locations are provided in Fig. 1 and Supplementary Table S1. Upon receipt, samples were immediately processed for total Hg (THg), methylmercury (MeHg), and bioavailable Hg, and aliquots were reserved for DNA extraction. All laboratory work began within 24 h of collection.

Our initial approach was to study the bacterial and fungal communities at only one time point in winter, and these samples were analyzed using 16S/ITS amplicon metagenomics and qPCR. Additionally, we got interested

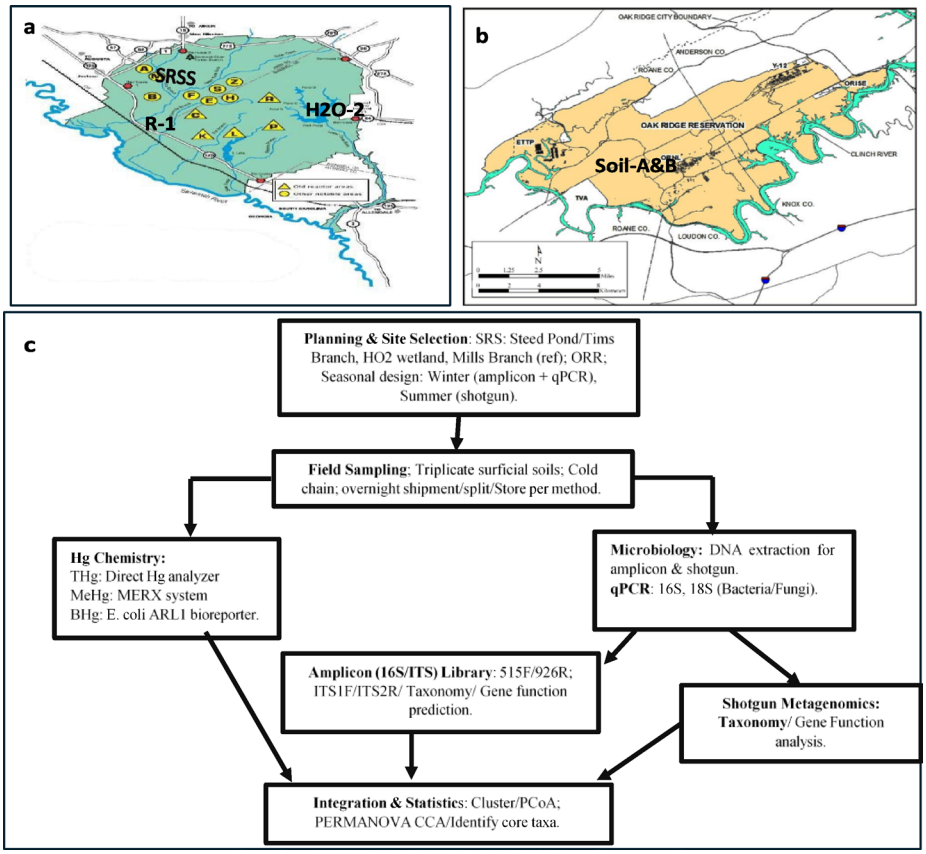

Fig. 1. The Integrated workflow for microbial community/functions profiling at two of the US metalliferous legacy sites. (**a**) the Savannah River Site (SRS), South Carolina, showing the SRSS, R-1, H2O-1, and H2O-2 sampling points (https://cntaware.org/wp-content/uploads/2020/02/2.20.20-UA-for-web.pdf); (**b**) The Oak Ridge Reservation, Tennessee, showing the sampling points (https://www.scirp.org/journal/paperinformation?paperid=103351); (**c**) The general workflow for community and functional profiling.

in the gene functions associated with the identified microbiomes after PICRUSt2 analysis on the 16S-based amplicon data and thus collected samples during the ensuing summer season for shotgun metagenomics. Thus, for seasonal comparisons, genomic DNA from both seasons and sites (SRS and ORR) were included in the shotgun metagenomics analysis.

Total Hg (THg), methyl Hg (MeHg), and bioavailable Hg (BHg)

THg was measured with a direct mercury analyzer (DMA-80) with atomic absorption detection, following previously described procedures[14]. Methylmercury (MeHg). MeHg was quantified using the MERX automated methylmercury system (Brooks Rand, Seattle, WA, USA) per the described method[14].

Bioavailable Hg was estimated using the mercury bioreporter *Escherichia coli* ARL1, which carries a chromosomal merR: luxCDABE fusion and produces light at Hg concentrations as low as 10 nM[24]. Cultures were grown at room temperature in minimal salts medium to OD600 = 0.2–0.3 before assay; luminescence measurements followed[29].

qPCR analysis

qPCR was performed in polypropylene 96-well plates in 25 µl reactions containing 12.5 µl qPCR master mix (ABgene), 1.25 µl each primer, 2.5 µl BSA (bovine serum albumin), 1.0 µl SYBR Green I, 1.0 µl ROX dye, 0.5 µl nuclease-free water, and 5 µl template DNA (0.5 ng μl^{-1}). Template DNA was extracted using the DNeasy PowerLyzer kit following the manufacturer's instructions (Qiagen, Germantown, MD, USA).

Primers for fungi were nu-SSU-0817 / nu-SSU-1196[30]; bacterial primers were Eub338 / Eub518. Thermal cycling conditions were: 95 °C for 15 min (initial denaturation), followed by 40 cycles of 95 °C for 60 s, 53 °C for 30 s, and 72 °C for 60 s. Each plate included triplicate reactions for each DNA sample and standards. Standard curves were prepared by cloning and purification of plasmid standards, followed by calculation of gene copy numbers[31].

Microbiome analysis

Soil genomic DNA was isolated using the DNeasy PowerLyzer kit (Qiagen). DNA quantity/quality was assessed with a NanoDrop micro-volume spectrophotometer. Samples were processed for amplicon (16S/ITS) and shotgun metagenomics as follows.

Libraries were prepared for 16S amplicon sequencing with the Illumina Nextera XT kit. Primers used were 515F/926R for Domain bacteria and[32] ITS1F/ITS2R[33] for Domain fungi. Sequencing was performed on an Illumina NextSeq 500 (2 × 150 bp, mid-output). Paired-end reads were merged with PEAR[34], trimmed to remove primers and ambiguous bases, and filtered at $p = 0.01$. The QIIME pipeline generated taxonomic summaries at sub-OTU resolution[35]. (Taxonomic assignment employed USEARCH against SILVA v132 (≥ 90% similarity) for 16S and UNITE for ITS[36,37]. Out of the three ORR soil samples, soilA did not yield publishable data so it was removed from the downstream analysis. PICRUSt2 (Phylogenetic Investigation of Communities by Reconstruction of Unobserved States)[38], was applied to 16S rRNA gene sequences to infer the functional potential of microbial communities, enabling prediction of gene family abundances and metabolic pathways across tested samples.

For shotgun metagenomics, equimolar libraries from high-quality DNA were prepared per Illumina protocols and sequenced on an Illumina HiSeq (2 × 150 bp). Reads were mapped to the NCBI non-redundant (NR) protein database using DIAMOND (default parameters;[39]). Taxonomic assignments were derived with MEGAN using the Least Common Ancestor (LCA) algorithm[40]. Relative abundances were computed from read counts. The SUPER-FOCUS pipeline was used to estimate gene and subsystem pathway abundances.

Metagenomic sequence accession numbers

Sequence data are available at NCBI SRA/ENA, accession SUB15225813, BioProject PRJNA1245361.

Statistical analysis

MicrobiomeAnalyst[41] was used on QIIME-processed data to identify the core microbiome and to perform diversity and differential-abundance analyses. α-diversity (Chao1; t test/ANOVA), β-diversity (PCoA on Bray–Curtis; PERMANOVA), and edgeR-based differential abundance (genus level; FDR-adjusted $p < 0.05$) were computed with built-in modules.

Canonical correspondence analysis (CCA) was conducted in CANOCO v5 (Microcomputer Power, Ithaca, NY, USA) to relate microbial communities to soil THg, MeHg and BHg data, following approaches shown to yield meaningful constrained ordinations for microbiological abundance data[42]. The integrated workflow for this study is shown in Fig. 1c.

To classify the environmental samples based on mercury concentrations, we employed a quantile-based statistical approach (https://pro.arcgis.com/en/pro-app/latest/help/mapping/layer-properties/data-classification-methods.htm). Specifically, the concentrations of total mercury (THg), bioavailable mercury (BHg), and Methylmercury (MeHg) were binned into three categories: low, medium, and high. For each mercury species, the dataset was sorted in ascending order, and the 33rd and 66th percentiles were calculated. These percentiles served as thresholds to define the three categories:

- Low: Values ≤ 33rd percentile
- Medium: Values between the 33rd and 66th percentiles
- High: Values > 66th percentile

This method ensures an even distribution of samples across categories and allows for relative comparison within the dataset. It is particularly useful when absolute regulatory thresholds are not applicable or when the goal is to explore internal patterns and variability in mercury speciation. Dendrogram analysis of the measured soil THg and MeHg concentrations from the SRS and ORR metalliferous sites was performed using the Primer-e software (https://www.primer-e.com/software).

Results and Discussion

Soil mercury measurements

Collected soils were analyzed for total mercury (THg) and methylmercury (MeHg). Based on the total Hg contamination levels, soils were divided into three (3) different categories: high, medium, and low (Table S1 and Fig. 2). Furthermore, to facilitate comparative analysis of mercury speciation across the tested samples, we categorized each sample based on the concentrations of three mercury forms: Total Mercury (Total Hg), Bioavailable Mercury (BHg), and Methylmercury (MeHg). The classification was performed using a quantile-based approach, which divides the dataset into three equal-sized groups corresponding to low, medium, and high concentration categories. It is noteworthy that using the quantile-based approach, only site SRSS-S2 was shown to be high using all three measurements of THg, BHg, and MeHg, respectively (Table S1).

Overall, the three soil samples obtained from the ORR ecosystem were found to be highest in total Hg concentration in comparison with the samples collected from SRS, hence were combined and categorized as 'high', with an average total Hg concentration of 2021 ppb. Samples obtained from SRSS1 and SRSS2 had the highest Hg concentration among the SRS samples, but lower than the ORR, and hence were categorized as 'medium', with an average of 847 ppb total Hg. SRS soil samples SRSS3 and SRSS4, along with HO2-1 and HO2-2, had considerably lower Hg contamination (62 ppb) and were categorized as 'low'. Uncontaminated soils collected from SRS were used as 'reference', with an average of 20 ppb Hg. The grouping of the samples according to the contamination levels can be found in the Supplementary Table S1.

Methylmercury (MeHg) was also analyzed for these soil samples and the highest concentration was found in the three ORR samples, followed by the soils marked as 'medium' based on THg (Fig. 2). The Lowest amount

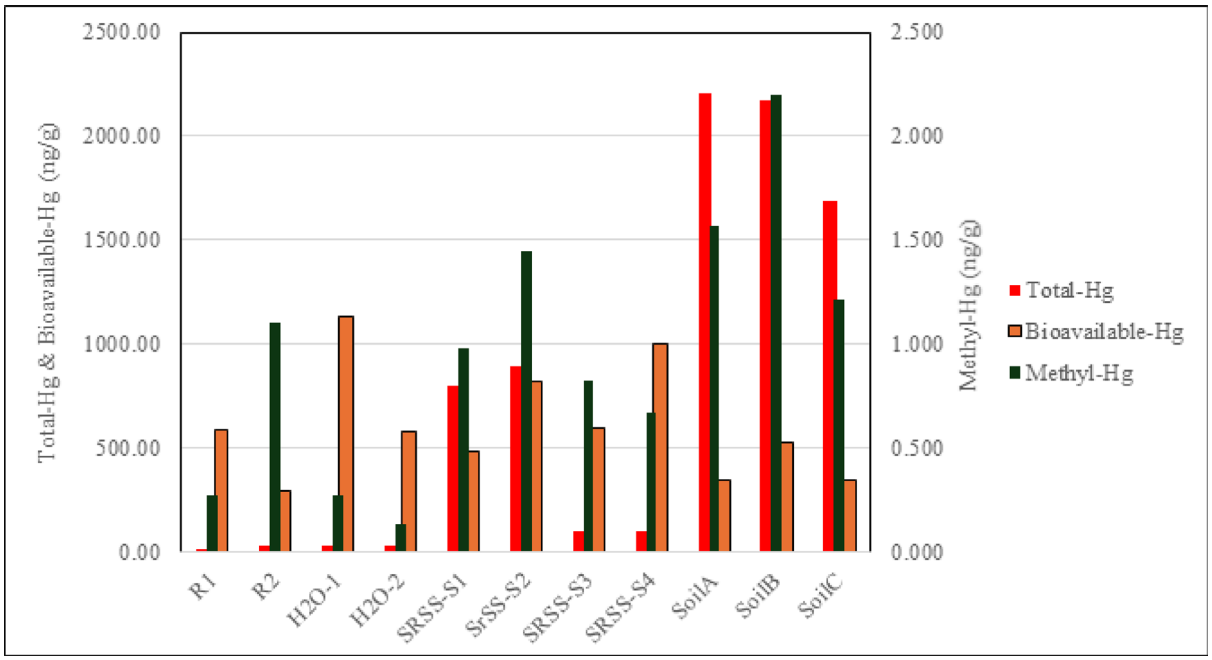

Fig. 2. Shown is the comparison of total mercury (THg), methylmercury (MeHg), and bioavailable mercury (BHg) in the SRS and ORR soils.

of MeHg was observed in the soils with 'low' THg. The amount of MeHg in 'low' soils was even lower than the amount of MeHg in the 'reference' soils with no apparent Hg contamination. In summary, the following trend was observed for MeHg concentration on soils: high > medium > reference > low (Supplementary Table S1). It should be noted that not much difference was observed in MeHg concentrations between 'high' and 'medium' soils. It was surprising to observe the high MeHg levels in the reference sample, relative to the 'low' Hg contaminated soils. Several factors influence the soil MeHg concentrations, such as the amount of carbon and nitrogen in the soils[20]. Higher carbon in the soil leads to higher binding of Hg to carbon and, in turn, can increase methylation rates[43].

Furthermore, when bioavailable Hg (termed as BHg) was measured for these soils using the *E. coli* ARL1 bioreporter strain, the highest bioavailability of mercury was found in the soils with low total Hg, followed by "medium" THg soils. Counterintuitively, the lowest BHg was present in soils with high total Hg. The amount of BHg in 'high' soils was even lower than the amount of BHg in the 'reference' soils with no apparent Hg contamination. The order of BHg was in the following order: low > medium > reference > high, based on THg concentration (Fig. 2). Hence, it should be noted that the total soil Hg is not reflective of the bioavailable Hg fraction, as bioavailability can be affected by several biogeochemical parameters, such as dissolved organic carbon and salinity[44]. In this context, it has been shown previously that bioavailable Hg can significantly differ from the total Hg concentration[45], where soils from two different regions in China were compared; this study found that bioavailable mercury in Wuhu samples was 0.0183% of the total Hg, while the bioavailable Hg in samples from Beijing was 0.296% of the total Hg. According to[46], the fraction of bioavailable mercury in a soil laden with high mercury contamination does not depend on the total mercury content of the soil; the bioavailable mercury varied indirectly with the organic carbon and the decreasing pH of the soil. In a similar experiment on the correlation between bioavailable mercury and total dissolved organic carbon,[47] reported that the dissolved organic carbon inhibited the mercury available for plant uptake, indicating the inverse relationship between the bioavailable mercury and the organic carbon contents of soil.

There have been a few studies at the SRS to define the bioavailable fraction of Hg in the SRS; however, they have used entirely different sets of parameters. For example, Hg in the tissues of wild animals in the area has been used to quantify bioavailable Hg[48], as also the method of using diffusive gradients in thin films (DGT) to estimate the labile Hg[13]. However, a comparison of the effect of total soil Hg on the bioavailable Hg fraction was not determined. Furthermore, bioavailable Hg concentrations determined in real time with a living organism-whole cell bioreporter system- is an important consideration in the soil assessment for contaminant levels and should be considered for future environmental assessments by regulatory agencies.

A dendrogram analysis of the measured soil THg and MeHg concentrations from the SRS and ORR metalliferous sites showed clustering of soils in four distinct groups- reference site (Mills Branch) clustered with site SRSS4 (Fig. S2). Interestingly, the highest contaminated sites—soil A, B, and C clustered separately from all other locations, likely due to the stress from long-term exposure to high mercury, thus affirming that the soil metal contamination level could potentially influence the site characteristics.

Microbial enumeration, taxonomy, and gene functions in Hg contaminated and uncontaminated sites

The first group of samples collected in the winter season was evaluated for bacterial and fungal gene copy numbers using the quantitative polymerase chain reaction (qPCR) technique and data is shown in Fig. S1a–d. The qPCR data generated using the universal bacterial primers were analyzed statistically, which resulted in an R^2 value of 0.99 and a slope of − 3.57 (data not shown). Highest bacterial numbers were present in the soil with a 'medium' level of Hg contamination; these numbers were at least one order of magnitude higher relative to soils labeled as 'high' and 'low'. Counterintuitively, the 'reference' uncontaminated soils showed lower gene copy numbers than the 'high' and 'low' soils, respectively (Supplementary Fig. S1). These results appear inconsistent with our overarching hypothesis that Hg contamination negatively impacts the soil microbial communities, such that microbial abundances will likely be higher in uncontaminated sites. We also determined the absolute and relative fungal gene copy numbers based on the 18S rRNA and ratios of the 16S:18S and vice versa (Supplementary Fig. S1). However, no significant correlation was apparent between the abundance of bacteria or fungi and soil Hg concentration. A similar observation has been reported before[49], where an insignificant relationship between total Hg and bacterial numbers based on qPCR was found. However, it remains unclear as to why we found lower bacterial numbers in the uncontaminated soil relative to the ones contaminated with Hg. One plausible explanation could be the presence of PCR inhibitors in some of these soil samples. According to[50], environmental samples are prone to PCR inhibition due to the strong affinity of clays and humic substances to DNA molecules, which will inadvertently stop the polymerase from completing amplification or will denature the polymerase[50].

The next part of this study was focused on the 16S amplicon and shotgun sequencing based metagenomics to evaluate the impacts of long-term Hg contamination and seasonal variations, respectively. It is noteworthy to state that combining 16S rRNA gene sequencing with shotgun metagenomic sequencing is widely recommended for environmental microbiome studies due to the complementary strengths of each approach. 16S amplicon sequencing efficiently profiles bacterial and archaeal community composition by targeting a conserved gene, offering genus-level taxonomic resolution and cost-effective insights into microbial diversity. However, it lacks functional information and can be biased by primer selection. Shotgun metagenomics, by contrast, can generate sequences of all DNA present in a sample, enabling species-and strain-level identification across all domains of life- including viruses and eukaryotes-while also revealing functional genes involved in biogeochemical processes, such as mercury detoxification via the *mer* operon. Moreover, this method captures rare or uncultured taxa and provides rich annotations of metabolic pathways, resistance genes, and ecological functions. Thus, using both techniques together facilitated this study to cross-validate taxonomic assignments, reduce methodological bias, and gain a holistic understanding of microbial structure and function in the complex SRS and ORR long-term metal-contaminated ecosystems.

Note that out of the three ORR soil samples, soilA did not yield publishable data so it was removed from downstream analysis. 16S-based amplicon analysis revealed Pseudomonadota, Chloroflexota, Bacteroidota, Acidobacteriota, and Verrucomicrobiota as the top five most abundant bacterial phyla in both SRS and ORR (Fig. 3a). Among the bacterial genera, the five most abundant ones were identified as *Spirochaeta*, *Geobacter*, *Flavobacterium*, *Syntrophorhabdus*, and *Anaeromyxobacter* (Fig. 3b), respectively. These results mirrored the shotgun sequencing data (Fig. 4a), such that again, the top five bacterial phyla were Pseudomonadota (~ 30–40%), Chloroflexota (~ 8–17%), Bacteroidota (5–15%), Acidobacteriota (~ 4–10%), and Verrucomicrobiota (~ 3–7%), regardless of the level of Hg contamination. However, the bacterial genus level communities in shotgun sequencing were identified as the *Bradyrhizobium*, Candidatus, *Geobacter*, *Pedosphaera*, and *Burkholderia*; the only common genera between amplicon and shotgun metagenomic analysis were *Burkholderia* species (Fig. 4b). Such anomaly between 16S and shotgun sequencing based taxonomic abundances is odd but not entirely unknown. Despite their widespread use in microbial community profiling, 16S rRNA gene sequencing and shotgun metagenomic sequencing often yield divergent estimates of bacterial genus-level abundance. These discrepancies arise from methodological and biological factors: (1) primer bias and gene copy variation: 16S sequencing is sensitive to primer mismatches and variable rRNA gene copy numbers across taxa, leading to over- or underrepresentation of certain genera[51,52]; (2) resolution and depth: Shotgun metagenomics offers higher taxonomic resolution and can detect rare or low-abundance taxa missed by 16S, but is more susceptible to host DNA contamination and extraction bias[53]; (3) taxonomic assignment algorithms: Differences in reference databases and classification pipelines contribute to inconsistent genus-level annotations[54]; (4) functional vs. taxonomic focus: While 16S targets conserved regions for taxonomic inference, shotgun sequencing captures functional genes, enabling broader ecological interpretation[55]. These methodological biases underscore the importance of integrative approaches and cautious interpretation when comparing microbial abundance across sequencing platforms. Emerging hybrid methods and standardized pipelines may help reconcile these differences in future studies.

Pseudomonadota, formerly known as Proteobacteria, are metabolically and ecologically diverse and are commonly found in many environments, including heavy metal-contaminated ecosystems[14,16,17]. Pseudomonadota likely play important functional roles in the SRS and ORR contaminated soils, such as bioremediation of heavy metals, nitrogen fixation, denitrification, and increasing soil nutrient availability (nutrient cycling)[56–58]. Other studies have also identified an increased abundance of Pseudomonadota in the presence of mercury contamination[58,59]. It was also observed that in Hg-contaminated soil, with changes in the microbial community, the relative abundance of strongly tolerant microorganisms increased, and sensitive microorganisms decreased[60]. The high dominance of Pseudomonadota in these soils may be facilitated by an extensive range of metal transport systems characteristic of this phylum[61]. Specifically, significant levels of heavy metal resistance have been observed in Pseudomonadota[62], most likely due to concrete efflux pumps regulating intracellular metal concentrations and facilitating cellular homeostasis and survival[63]. Genes (*tet* (B, C, or K), *mepA* (4%), *mdeA, norA, norB, and norC,* etc. encoding efflux proteins have been observed in Pseudomonadota

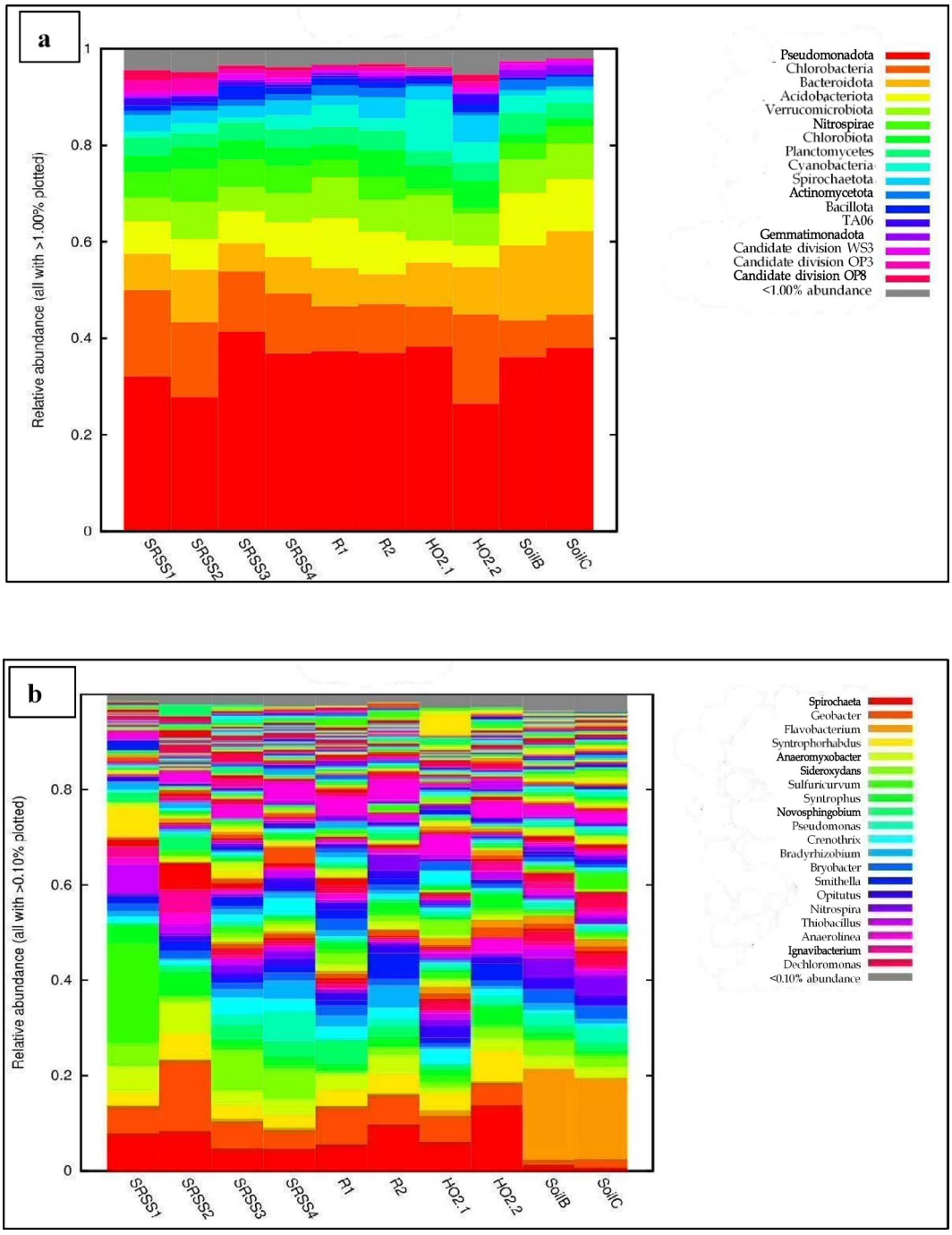

Fig. 3. The bar plot of bacterial abundance based on the 16S amplicon sequencing of the soil samples collected at different points from the SRS and ORR ecosystems. Out of the three ORR soil samples, soilA did not yield publishable data so it was removed from downstream analysis. (**a**) shows the phylum-level bacterial abundance, indicating that Pseudomonadota, Chloroflexota, Bacteroidota, Acidobacteriota, and Verrucomicrobiota were the five most abundant bacteria in both SRS and ORR; (**b**) shows the genus bacteria abundance, indicating that the five most abundant bacterial genera were *Spirochaeta*, *Geobacter*, *Flavobacterium*, *Syntrophorhabdus*, and *Anaeromyxobacter,* respectively.

even when they were not exposed to high concentrations of heavy metals[64]. Genomic studies have confirmed the presence of an array of heavy metal resistance genes in Pseudomonadota[65]. Our previous studies also align with the well-known traits of Pseudomonadota, such as bioremediation of heavy metals and nutrient cycling[14]. Bacteroidota was strongly associated with Hg concentrations in both samples. In contrast, the association of Chloroflexota and Hg concentration was more apparent in the SRS samples, with a lower mercury concentration than the ORR samples (Fig. 3a).

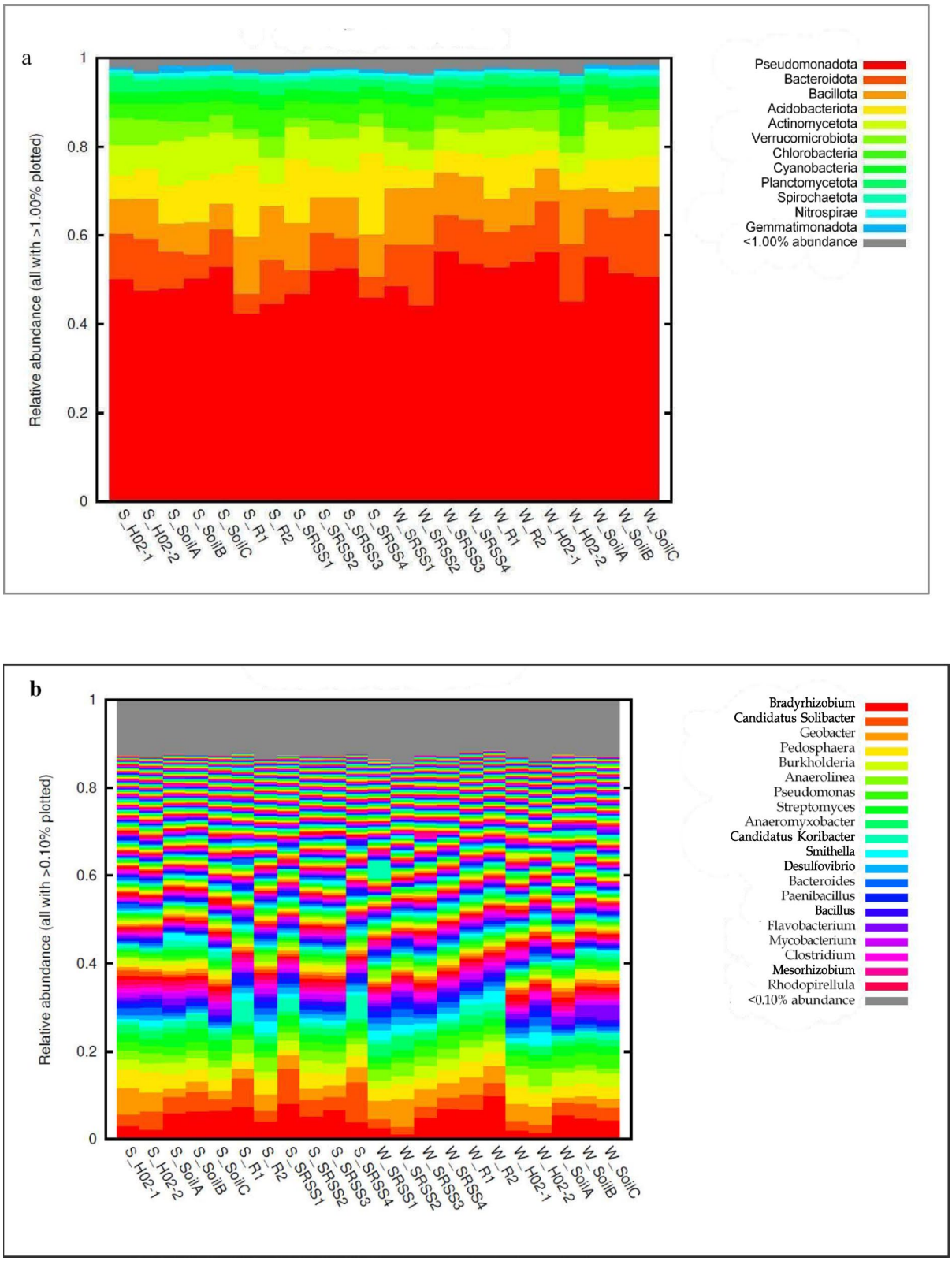

Fig. 4. The bar plot of bacterial abundance based on the shotgun sequencing of the soil samples collected at different points from the SRS and ORR ecosystems. (**a**) shows the phylum-level bacterial abundance, indicating Pseudomonadota, Bacteroidota, Bacillota, Acidobacteriota, and Verrucomicrobiota as the six most abundant bacteria, most of which coincide with the amplicon sequencing result; (**b**) shows the genus-level bacteria abundance, indicating the prevalence of *Bradyrhizobium*, Candidatus, *Geobacter*, *Pedosphaera*, and *Burkholderia*.

Regardless of contamination levels, the other dominant phyla in this study were Chloroflexota, Bacteroidota, Acidobacteriota, and Verrucomicrobiota, which have all been positively correlated with heavy metal contamination. In a previous study, the Chloroflexota phyla was considered to serve as a good bioindicator for the presence of Hg[65]. Similarly, Bacteroidota has been shown to thrive in Hg-contaminated soils[66]. Our findings further revealed the strong association of Hg and Bacteroidota, indicating that this group could be an appropriate target for further studies of Hg remediation in the SRS and ORR ecosystems (Fig. 3a).

Predominant bacterial genera identified across the tested soils belonged to *Bradyrhizobium*, *Geobacter*, *Pedosphaera,* and *Burkholderia* (Fig. 3b). Many of these bacterial groups, in particular *Bradyrhizobium* and *Burkholderia,* have been extensively found in our previous cultivation-dependent or cultivation-independent studies on the SRS and ORR soils[14,16,17]; lending further credibility for these groups to be the "core" groups of bacteria for SRS and ORR habitats and render critical ecosystem-level services such as metal detoxification and cycling of nutrients[14]. In our genomics-based studies conducted on mercury resistant bacteria, we found several interesting traits harbored in the genomes of SRS and ORR native *Bradyrhizobium* and *Burkholderia* species, in that they possess a plethora of multiple efflux pumps and membrane transporters for providing resistance to heavy metals[18,67], thus facilitating their growth and proliferation within contaminated soils. Furthermore, *Geobacter* has been shown to adsorb Hg on its surface and participate in the reduction of Hg (II) to Hg (0)[68], thus indicating the role of *Geobacter* in Hg recycling. Such studies from the SRS and ORR soils will likely pave the way for precise bioremediation, restoration, and management of these long-term legacy contaminated habitats.

Although not belonging to the predominant "core" bacterial groups identified in metagenomic studies, interesting genome-enabled traits have been found in mercury resistant bacterial isolates native to the SRS and ORR ecosystems. Specifically, we confirmed the presence of a complete *mer* operon comprising of *merA* (mercuric reductase), *merB* (organomercurial lyase), and associated regulatory genes in *Arthrobacter* sp. H-02–3[14]. In this study, functional analysis suggested a two-step detoxification pathway wherein *merB* cleaves methylmercury (MeHg) to Hg^{2+}, which is subsequently reduced to volatile Hg^{0} by *merA*, thereby mitigating toxicity in situ. In another study, we applied the metagenome assembled genome (MAG) technique to shotgun metagenome sequences obtained the SRS soils; the *Arthrobacter* MAG emerged as particularly robust, with 1,749 genes linked to nitrogen, phosphorus, and sulfur metabolism, and 598 genes encoding enzymes for resistance to metals such as cadmium, zinc, chromium, arsenic, and copper[69] Despite the suitability of such organisms for mercury bioremediation, we provide caution because long-term exposure to heavy metals can also promote recruitment of antimicrobial resistance genes (AMR) in the native microbiota. As an example, in *Arthrobacter* sp. H-02–3, we identified a suite of genes conferring resistance not only to mercury (e.g., merA, merB) but also to other heavy metals and multiple antibiotics. The presence of antimicrobial resistance (AMR) genes alongside bioremediation-relevant traits raises concerns about the unintended ecological risks of deploying such bacteria in environmental cleanup efforts. Therefore, we emphasize the need for careful screening of microbial strains used in bioremediation, particularly in ecosystems already burdened by metal contaminants, to avoid exacerbating AMR dissemination.

In a separate study, *Stenotrophomonas* sp. MA5, also isolated from SRS, demonstrated rapid mercury volatilization and resistance[11]. Whole genome sequencing revealed a transposon-derived *merRTPADE* operon, with qRT-PCR confirming ~ 40-fold upregulation of *mer* genes upon Hg^{2+} exposure. This strain depleted over 90% of spiked Hg^{2+} within 24 h, highlighting its bioremediation potential. However, both strains exhibited co-occurrence of metal resistance genes (MRGs) and antibiotic resistance genes (ARGs), suggesting environmental co-selection pressures and underscoring the ecological relevance of *mer*-operon-bearing microbes in long-term contaminated habitats.

To further probe the Hg-cycling microbiota in sites containing variable levels of Hg contamination, we collected another set of samples in the summer season to check how seasonality impacts the community structure of bacterial and fungal groups within the SRS and ORR soils. Mirroring the amplicon-based results, Pseudomonadota was again identified as the most abundant phylum (~ 43–50%), irrespective of the level of Hg contamination and the sampling season. Other bacterial phyla found in the order of their abundance were Bacteroidota (~ 5–15%), Bacillota (~ 5–15%), Acidobacteriota (~ 5–15%), Actinomycota (~ 5–10%), and Verrucomicrobiota (~ 5–10%) (Fig. 4a). In comparison to the other soil groups, the 'high' contamination group had a relatively higher abundance of Bacteroidetes (Figs. 3a and 4a). Bacteroidetes grown in the presence of Hg have been shown to volatilize it[70]; hence, their resistance to higher concentrations of Hg can be expected. Relatively higher concentrations of Bacillota were observed in the 'medium' soils (Fig. 4a); Hg-resistant Bacillota from Oak Ridge soils have been previously isolated and have been shown to resist four µg/ml Hg. However, they did not contain *mer*A genes[71].

It has previously been shown that sequencing strategies can significantly impact environmental metagenome surveys[72]. For example, in the analysis of the human gut microbiome[73], it was found that deeper characterization of the microbiome complexity was obtained by shotgun sequencing, thus allowing for the identification of a larger number of species when compared to 16S amplicon sequencing. In this present study, we also observed a disconnect between genus-level microbiomes identified by the amplicon and shotgun-based approach, such that the predominant bacterial genera identified across all the tested soils mainly belonged to *Bradyrhizobium*, *Candidatus, Geobacter*, *Pedosphaera,* and *Burkholderia,* irrespective of the soil contamination level (Fig. 4b). As stated for the amplicon sequencing result, *Bradyrhizobium* and *Burkholderia* likely are the "core" groups of bacteria in the SRS and ORR ecosystems and are primarily responsible for providing critical ecosystem-level services[18,67]. These results also align with other studies, which have unequivocally demonstrated the presence of Hg-resistant *Bradyrhizobium* strains from heavy metal-contaminated soils[74,75]. It has also been shown that *Bradyrhizobia* positively impacts legumes grown in high mercury-contaminated soils and provide plant growth-promoting activities by reducing Hg toxicity[76]. *Geobacter* numbers were relatively higher in the 'medium' contaminated soils, and it is a possibility that *Geobacter* sp. could be metabolically active to facilitate

the formation of MeHg[77]. An additional attribute to *Burkholderia* spp. as the "core" bacterial group in SRS and ORR soil habitats emerges from the ability of this group to reduce Hg(II) to Hg(0) and/or degrade MeHg[78].

One additional and critical goal of this study was to investigate the structure and functions of fungi in both SRS and ORR ecosystems, stemming from the fact that fungi can outcompete bacteria under higher levels of heavy metal stress[19,79]. Regardless of contamination level or seasons, *Ascomycota* was the dominant fungal phylum, followed by Basidomycota (Fig. 5a)-a finding in line with our previous study[14]. A similar observation of dominance of *Ascomycota* has also been reported in Hg contaminated soils from the former mercury mining plant in Rudňany in central Slovakia[21], as well as another study on different heavy metal contaminants[80]. Since the Ascomycota phylum contains saprophytic fungal species with a unique ability to recycle even recalcitrant compounds, including lignin and keratin, it can be hypothesized that Ascomycota possesses stronger environmental adaptability, which enabled this phylum to be ubiquitous in contaminated metalliferous soils studied herein. Isolation and genomic analyses of fungal isolates from Hg contaminated sites have shown a variety of genes responsible for environmentally, ecologically, and evolutionary beneficial traits, such as heavy metal resistance, membrane transport, efflux, as demonstrated for other metal contaminated ecosystems[81], thus providing one reasoning behind finding this phylum at more than 70% of the total relative abundance in the SRS and ORR soils.

At the genus level, *Fusarium, Pseudogymnoascus* and *Aspergillus* were observed to be dominant (Fig. 5b). Note that all these three fungal genera belong to the Ascomycota phylum and were also reported in our previous study, which utilized diffusion chambers (DC) and microbial traps (MT) to enrich and assess these communities from the SRS and ORR soils[16]. *Fusarium* strains have been shown to resist metals and be agents of environmental detoxification associated with metals[82]. Similarly, *Aspergillus* isolated from Hg-contaminated environments was shown to resist up to 100 ppm of Hg[83]. Several species of *Aspergillus* have also been shown to absorb significant amounts of Hg on their surface, thus reducing the mercury concentration in contaminated environments[84]. In certain conditions, *Aspergillus* has also demonstrated the capability to biosorb MeHg; however, at a lower rate than Hg[85]. However, not much is known about the ability of fungal strains to contribute to Hg bioremediation, and it would be of significant interest to isolate these fungal members and evaluate their range of bioremediation potential. Overall, it can be concluded that these fungal genera have recruited ecologically beneficial traits to facilitate their colonization and survival within the tested metalliferous soils.

Statistical evaluation of bacterial and fungal communities with site environmental measurements

Differences between the α- and β-diversity of soil microbiomes across the SRS and ORR habitats were further evaluated and ordinations plotted as PCoA using the Bray–Curtis index. The α-diversity refers to the diversity of species within a single sample, while the β-diversity measures the diversity between two or more sample sets. Figure 6 represents the α-diversity plots for the bacterial and fungal communities in the contaminated soils. The order of α-diversity observed at the bacterial phylum level was in order: Reference > Medium ~ Low > High (Fig. 6a). Higher diversity was found in the 'low' Hg contaminated site, probably due to the selection of several strains since the toxicity level of Hg was not too high. The bacterial genus level α diversity was similar for all the contamination levels except for 'high', probably due to the selective pressure posed by soil mercury and other contaminants (Fig. 6b). In case of fungi, the α-diversity followed similar trends at both phylum (Fig. 6c) and genus levels (Fig. 6d). In both cases, α-diversity was similar at all the contamination levels except at the 'low' Hg contamination level, which was very diverse. As discussed above, since fungi are also sensitive to higher concentrations of environmental contaminants, the possibility of their proliferation at low toxic levels of Hg seems to be well supported.

To further test which of the measured environmental factors shaped the bacterial and fungal diversity in the SRS and ORR Hg-impacted soils, Canonical Correspondence Analysis (CCA) was performed using the top five bacterial and fungal genera along with the total Hg, MeHg, and Bioavailable Hg. As shown in Fig. 7a, Pseudomonadota and Actinomycota were influenced significantly by THg and MeHg, whereas Bacillota were associated with low levels of THg and MeHg and high levels of Bioavailable Hg. At the genus level, *Burkholderia* showed a strong correlation with THg. At the same time, *Candidatus* Solibacter was strongly affected by bioavailable Hg (Fig. 7b). As stated above, *Burkholderia* spp. have been found in SRS, ORR, and also the Old Rifle Processing DOE Site in Colorado[86]. Our previous experiments on the heavy metal-contaminated SRS soils have also led to the isolation of several *Burkholderia* spp.[14,67], providing a strong basis for targeting *Burkholderia* in bioremediation studies at DOE metalliferous soils. In the case of Fungi, phylum-level analysis showed Ascomycota and Basidomycota to exert strong correlations with THg and MeHg (Fig. 7c). Overall, it can be stated that THg and MeHg showed a cumulative effect in shaping the overall bacterial and fungal diversity in the two DOE legacy contaminated sites studied herein.

Functional metagenomics

Fundamental understanding of microbially-mediated functions for heavy metal remediation in former US DOE legacy contaminated sites remains understudied. Hence, to infer functional and metabolic responses of microbial communities across different Hg contaminated sites, we first performed PICRUSt2 analysis on the 16S-based amplicon data. PICRUSt2 is an integrated resource, based on the KEGG database, comprising 15 manually curated databases under BRITE and PATHWAY categories. The top category in the BRITE bacterial-based analysis was transporters, which seemed to be predominant across all the soils irrespective of the Hg contamination level (Fig. 8a), indicating that microbial communities likely use the cellular transport function to survive in metalliferous soils. The number of transporters was similar in all the soils except for the medium contaminated sites-SRSS1 and SRSS2. Furthermore, the top categories in the PATHWAY analysis were metabolic pathways, biosynthesis of secondary metabolites, and metabolism in diverse environments (Fig. 8b).

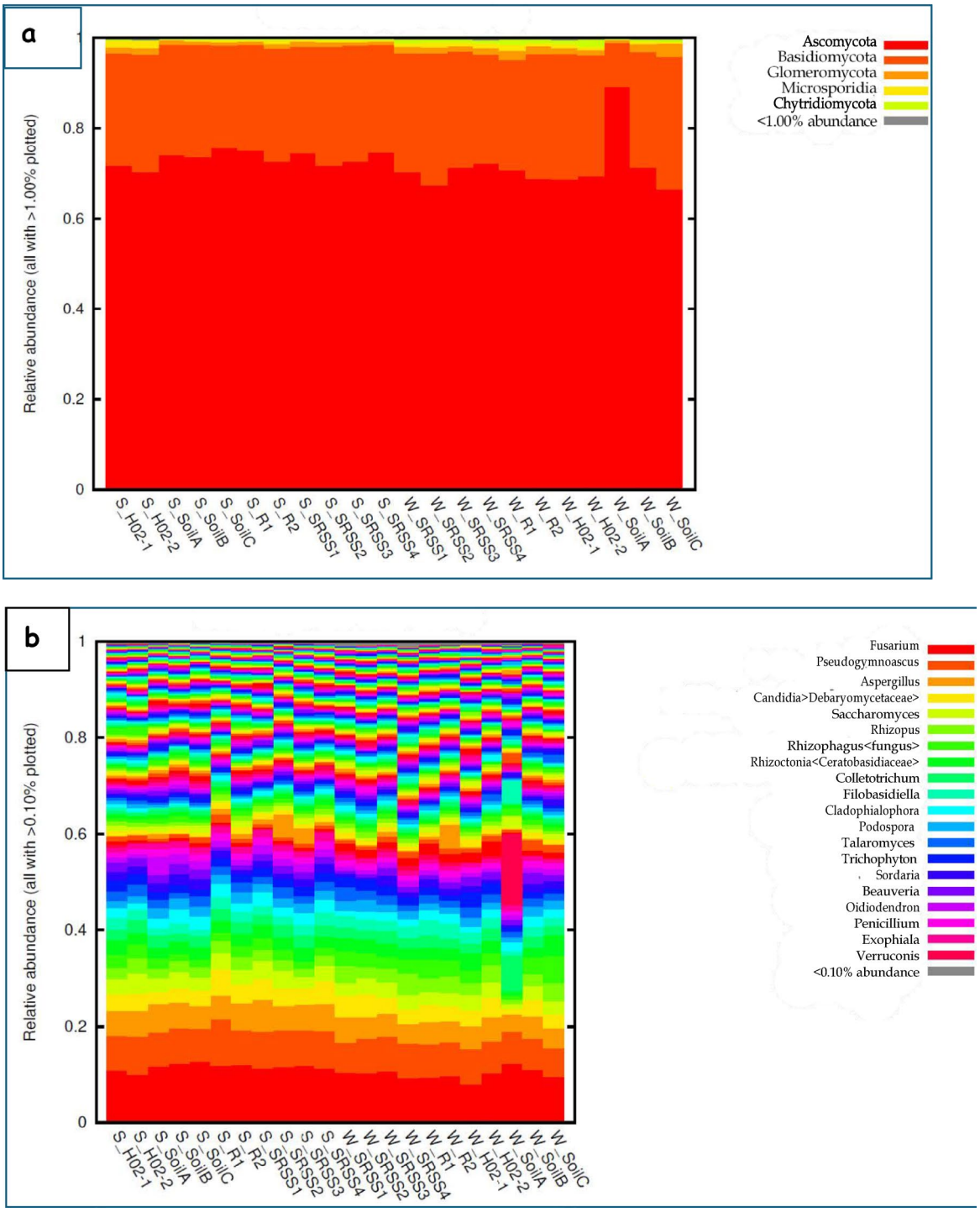

Fig. 5. The fungal relative abundance based on the shotgun sequencing of the soil samples collected at different points from the SRS and ORR ecosystems. (**a**) shows the phylum-level fungal abundance, indicating that Ascomycota was the dominant fungus, followed by *Basidomycota,* irrespective of the Hg contamination level and the sampling season; (**b**) shows the genus-level fungal abundance, indicating that Fusarium, Pseudogymnoascus, and Aspergillus were the most abundant genera across the sampling sites, contamination levels, and seasons.

We also investigated whether bacterial and fungal taxonomic shifts between contaminated and non-contaminated SRS and ORR soils were also evident at the gene functional levels. To address this, function-level analysis at the subsystem level 1 on the shotgun sequence data showed genes functions related to carbohydrate metabolisms, protein metabolism, respiration, and virulence to be abundant. Among the primary gene functions, stress response and membrane transport were also present in all the soils (Fig. 9a). Note that membrane

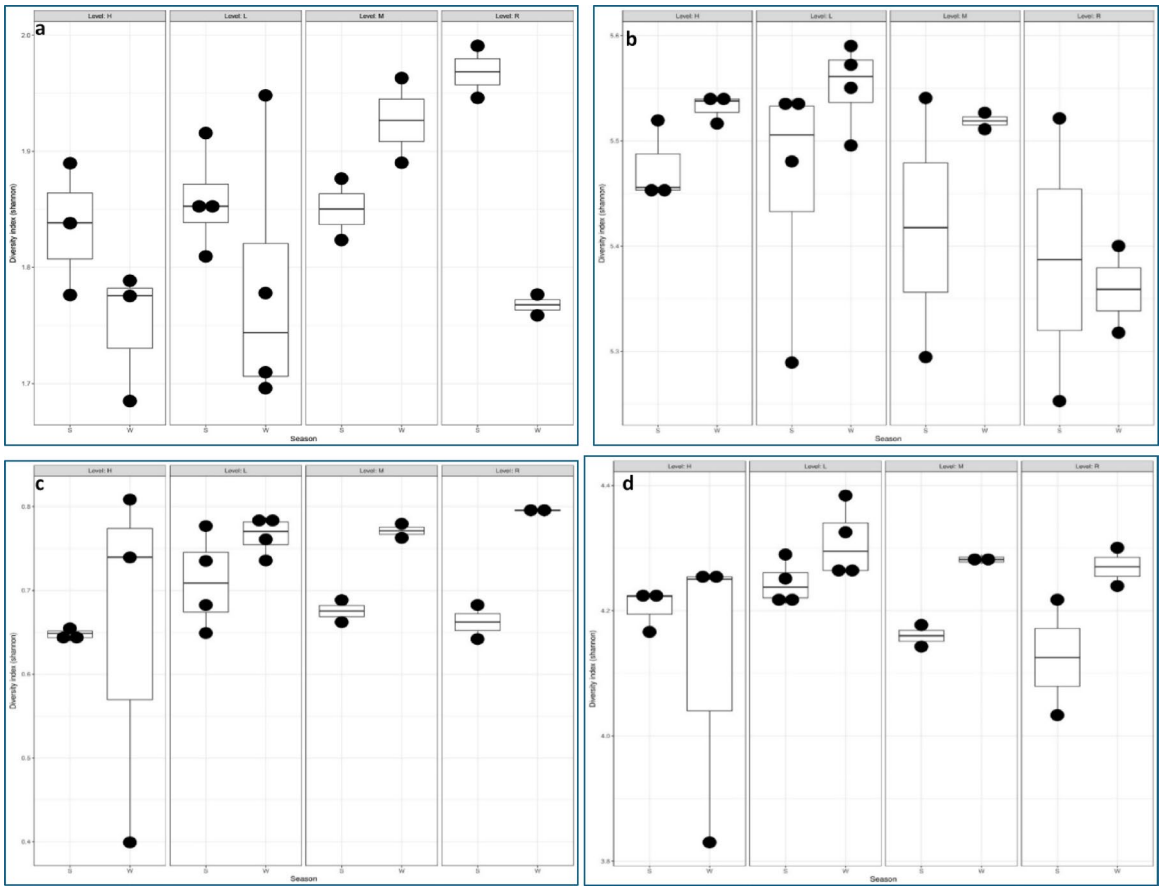

Fig. 6. The alpha diversity of the bacterial and fungi in the SRS and ORR Hg contaminated sites based on the shotgun sequencing grouped by the level of contamination and the sampling season. For bacteria at the phylum level (**a**), the order of diversity with respect to the level of contamination was R > M > L > H. These abbreviations pertain to levels of mercury contamination- R (Ref), M (middle), L (low) and H (high), respectively. The highly contaminated sites were less diverse due to Hg toxicity. For the seasonal consideration, the average median diversity index of the S samples was higher than that of the W samples. However, the average maximum diversity indices of the two groups were not significantly different. At the genus level (**b**), the "low" mercury contaminated samples had the highest bacterial diversity index, but the average maximum diversity indices of the samples were not substantially different from each other. For the fungi at phylum level (**c**), the average median diversity indices of the samples based on the contamination levels were almost the same except the "high" sample which was substantially lower. The average maximum diversity indices based on the sampling season indicates that the W samples were more diverse than the S samples. At the genus level (**d**), the average median diversity indices based on the level of contamination were almost equal, but the average maximum diversity of the "low" sample was higher than the rest. Based on the sampling season, the W samples were more diverse than the S samples.

transport is a critical feature for membrane-dependent heavy metal transport by soil-borne bacteria and is likely the mechanism for native microbiota to deter heavy metal toxicity[14]. Moreover, inorganic Hg(II) is transported into microbial cells via transporters, through the ion transport system, and methylated to MeHg intracellularly[87].

Gene functions at the subsystem level 2 were dominated by carbohydrate metabolism and protein biosynthesis functions across the tested soils. It is noteworthy that the fourth most abundant gene function in these Hg contaminated soils was for resistance to antibiotics and toxic compounds (Fig. 9b). The nexus between heavy metals and the exacerbation of antimicrobial resistance is well known, including our previous studies on isolated strains representative of the SRs and ORR contaminated habitat[18,67]. Moreover, at subsystem level 3, the YgfZ gene family, along with the cobalt-zinc-cadmium resistance genes, were identified, which are well known to facilitate bioremediation of contaminants (Fig. 9c). Specifically, the YgfZ proteins are responsible for the assembly or repair of iron/sulfur clusters that actively participate in several cellular processes such as catalysis, electron transport, gene regulation, DNA replication and repair, and central metabolism[88].

Conclusions

This study provides a comprehensive assessment of bacterial and fungal community structure, diversity, and functional potential across gradients of mercury contamination at two historically impacted U.S. Department of Energy sites—Savannah River Site (SRS) and Oak Ridge Reservation (ORR). By integrating qPCR, amplicon

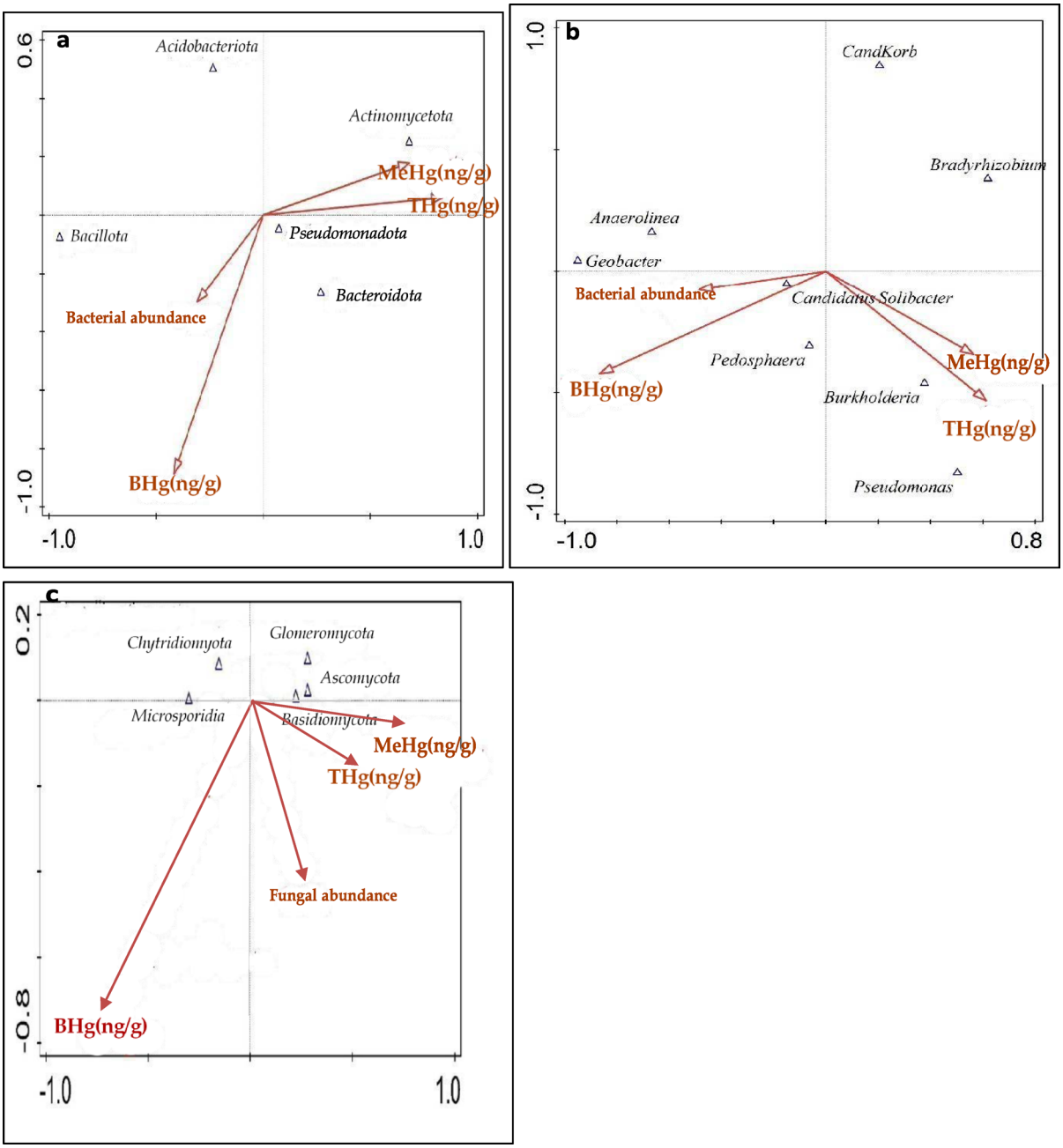

Fig. 7. The Canonical Correspondence Analysis (CCA) of the most abundant bacterial and fungi identified from the SRS and ORR Hg contaminated sites, based on the shotgun sequencing, with respect to the total mercury (THg), methyl mercury (MeHg), bioavailable mercury (BHg), and gene copy numbers of total soil bacteria (16S) and total soil fungi (18S) from qPCR analysis. For bacteria at phylum level (**a**), Actinomycetota, Pseudomonadota, *and* Bacteroidota were positively associated with the THg, and MeHg, while the Bacillota were positively associated with the BHg. At the genus level (**b**), *Burkholderia* and *Pseudomonas* were positively associated with THg and MeHg, while *Pedospaera* and Candidatus *Solibacter* were positively associated with BHg. For fungi (**c**), Ascomycota and Basidomycota, the two most dominant phyla, were positively associated with THg and MeHg, while Blastocladiomycota was positively associated with BHg.

sequencing, and shotgun metagenomics, we demonstrate that long-term mercury exposure alters microbial community composition and functional gene repertoires, with bacterial α-diversity declining under high Hg stress while fungal diversity remains comparatively stable. Canonical correspondence analysis revealed distinct taxon–mercury speciation linkages, and functional profiling identified consistent enrichment of stress-response genes, membrane transporters, and phosphate metabolism pathways in contaminated soils. Notably, bioavailable mercury did not correlate directly with total Hg levels, underscoring the importance of speciation in microbial exposure and ecological risk assessment. The detection of resilient microbial taxa and pathways relevant to

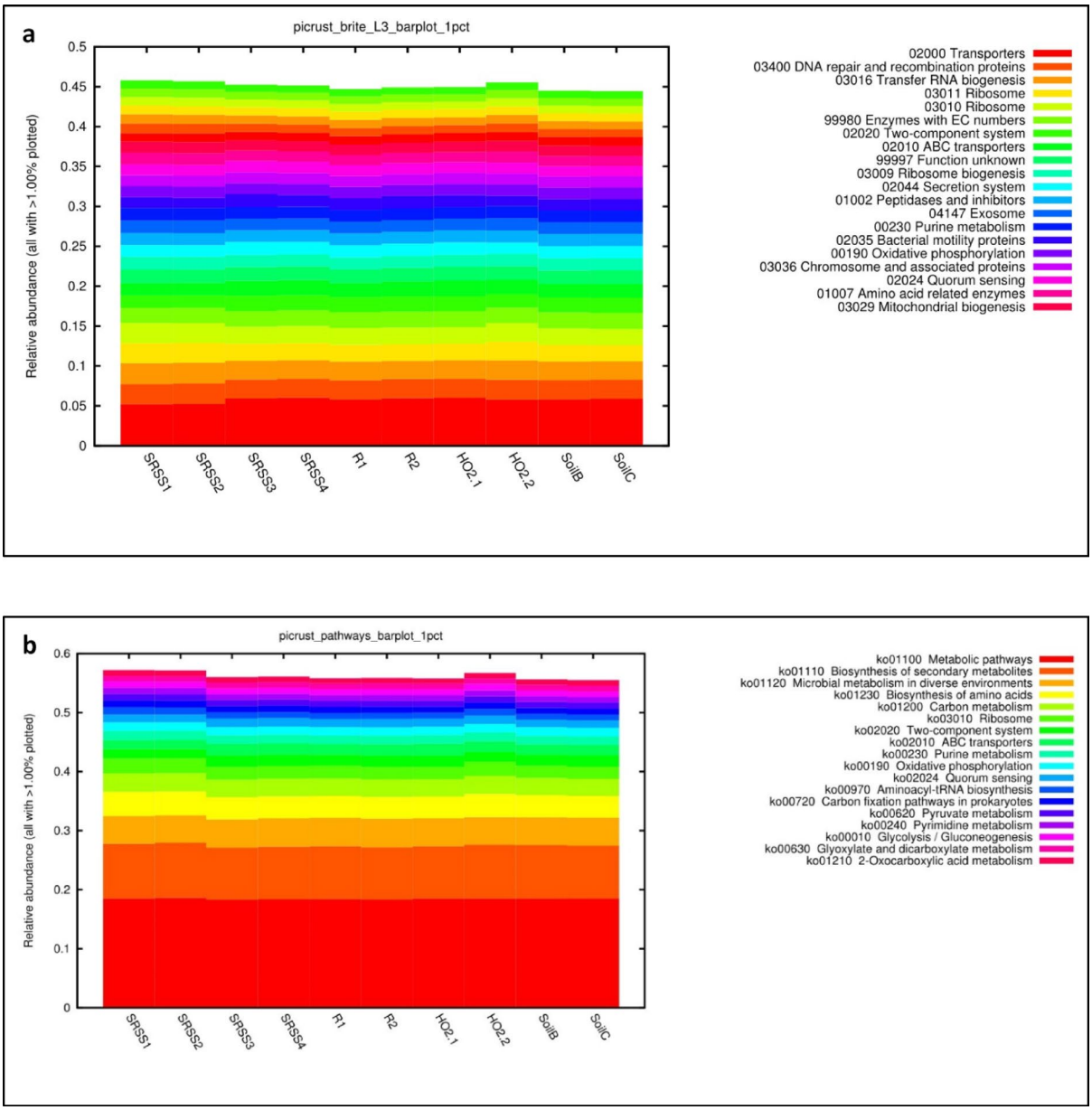

Fig. 8. PICRUSt2 analysis on the 16S amplicon data provided and indication of the microbiomes functional profiles in the SRS and ORR Hg contaminated soils based on the KEGG BRITE hierarchy (**a**) and KEGG Pathway (**b**).

mercury detoxification and nutrient cycling highlights the adaptive plasticity of native microbiomes and their potential role in bioremediation. These findings advance our understanding of cross-kingdom microbial responses to heavy metal stress and offer valuable insights for future restoration strategies at legacy-contaminated sites.

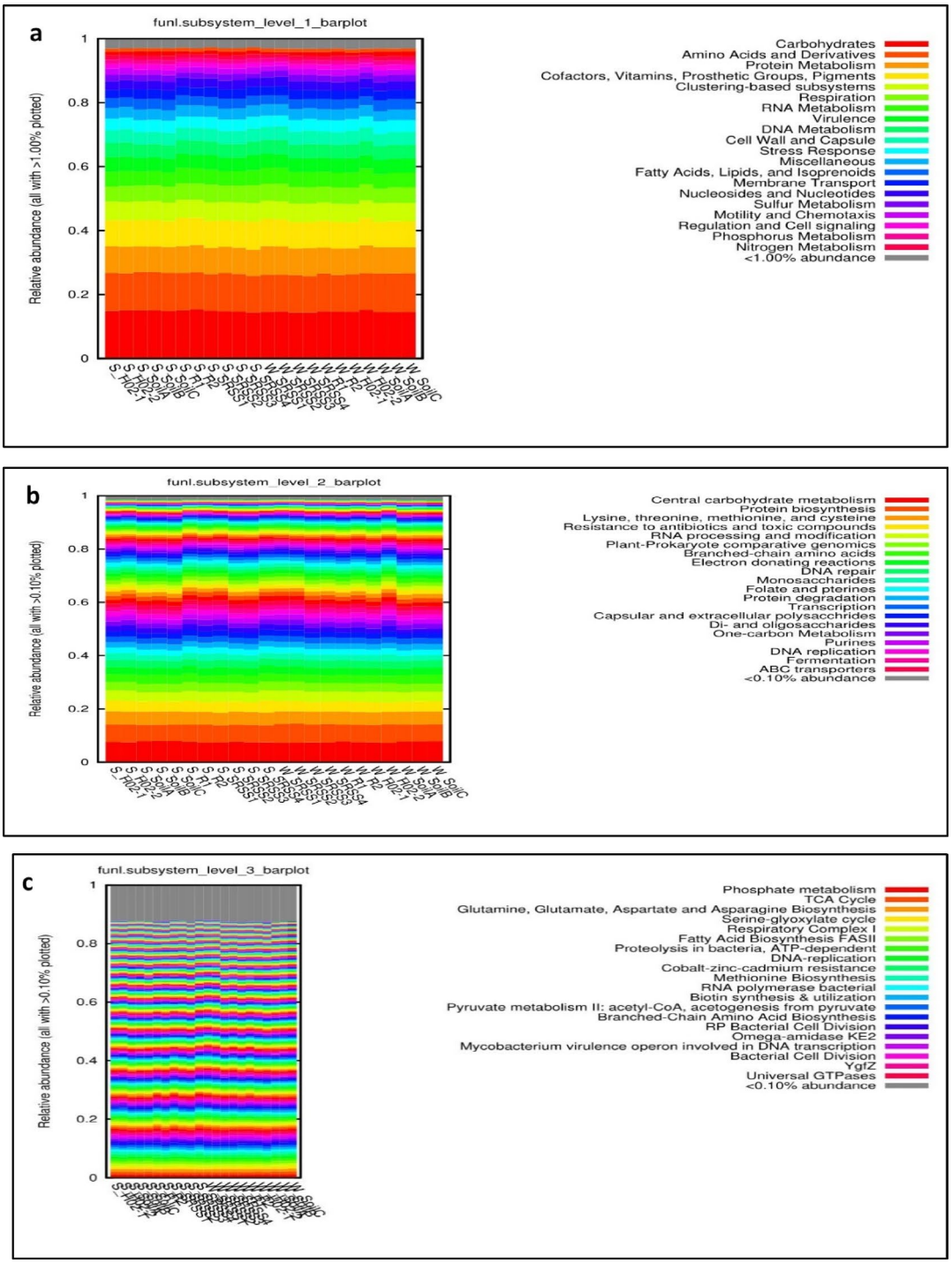

Fig. 9. The shotgun metagenome profile of the SRS and ORR Hg contaminated soils using the MG-RAST at different subsystem levels. At subsystem level 1 (**a**), genes encoding for carbohydrate metabolism, amino acid and derivatives, and protein metabolism were the most dominant irrespective of the contamination level and the sampling season. At subsystem level 2 (**b**), genes encoding for central carbohydrate metabolism, protein biosynthesis are the most dominant. At subsystem level 3 (c), genes for phosphate metabolism and the TCA cycle predominated.

Data availability

Metagenomic sequence accession numbers obtained from this study are available at NCBI SRA/ENA, accession SUB15225813, BioProject PRJNA1245361 (https://www.ncbi.nlm.nih.gov/bioproject/?term = PRJNA1245361).

Received: 9 April 2025; Accepted: 25 October 2025

Published online: 25 November 2025

References

1. World Health Organization. Mercury and health. https://www.who.int/news-room/fact-sheets/detail/mercury-and-health (2023).
2. Kumar, V., Tyagi, S., Kumar, K. & Parmar, R. Heavy metal-induced environmental pollution through waste disposal. *Internat. J. Res. Publicat. Rev.* **4**, 1205–1210 (2023).
3. O'Connor, D. et al. Mercury speciation, transformation, and transportation in soils, atmospheric flux, and implications for risk management: A critical review. *Environ. Internat.* **126**, 747–761. https://doi.org/10.1016/j.envint.2019.03.019 (2019).
4. Ke, T. et al. Epigenetics and methylmercury-induced neurotoxicity: evidence from experimental studies. *Toxics.* **11**(1), 72. https://doi.org/10.3390/toxics11010072 (2023).
5. Charkiewicz, A. E., Omeljaniuk, W. J., Garley, M. & Nikliński, J. Mercury exposure and health effects: what do we really know?. *Int. J. Mol. Sci.* **26**(5), 2326. https://doi.org/10.3390/ijms26052326 (2025).
6. Bose-O'Reilly, S., McCarty, K. M., Steckling, N. & Lettmeier, B. Mercury exposure and children's Health. *Curr. Problems Pediatric Adolescent Health Care* **40**(8), 186–215. https://doi.org/10.1016/j.cppeds.2010.07.002 (2010).
7. Hong, Y. S., Kim, Y. M. & Lee, K. E. Methylmercury exposure and health effects. *J. Prev. Med. Public Health* **45**(6), 353–363. https://doi.org/10.3961/jpmph.2012.45.6.353 (2012).
8. Pathak, A., Anjaria, P., Bhavsar, P.& Asediya, V. Health risk linked to mercury toxicity in food and environment. In: Kumar, N. (eds) Mercury Toxicity Mitigation: Sustainable Nexus Approach. *Earth and Environmental Sciences Library.* (Springer, Cham, 2024) https://doi.org/10.1007/978-3-031-48817-7_6
9. Boyd, E. & Barkay, T. The mercury resistance operon: from an origin in a geothermal environment to an efficient detoxification machine. *Front. Microbiol.* **3**, 33236. https://doi.org/10.3389/fmicb.2012.00349 (2012).
10. Priyadarshanee, M., Chatterjee, S., Rath, S., Dash, H. R. & Das, S. Cellular and genetic mechanisms of bacterial mercury resistance and their role in biogeochemistry and bioremediation. *J. Hazardous Mater.* https://doi.org/10.1016/j.jhazmat.2021.126985 (2022).
11. Agarwal, M., Rathore, R. S., Jagoe, C. & Chauhan, A. Multiple lines of evidence reveal mechanisms underpinning mercury resistance and volatilization by Stenotrophomonas sp MA5 isolated from the Savannah River Site (SRS) USA. *Cells* **8**(4), 309. https://doi.org/10.3390/cells8040309 (2019).
12. Podar, M. et al. Global prevalence and distribution of genes and microorganisms involved in mercury methylation. *Sci. Adv.* https://doi.org/10.1126/sciadv.1500675 (2015).
13. Xu, X., Bryan, A. L., Mills, G. L. & Korotasz, A. M. Mercury speciation, bioavailability, and biomagnification in contaminated streams on the Savannah River Site (SC, USA). *Sci. Total Environ.* **668**, 261–270. https://doi.org/10.1016/j.scitotenv.2019.02.301 (2019).
14. Pathak, A. et al. Characterization of bacterial and fungal assemblages from historically contaminated metalliferous soils using metagenomics coupled with diffusion chambers and microbial traps. *Front. Microbiol.* **11**, 1024. https://doi.org/10.3389/fmicb.2020.01024 (2020).
15. Vishnivetskaya, T. A. et al. Microbial community changes in response to ethanol or methanol amendments for U(VI) reduction. *Appl. Environ. Microbiol.* **76**, 5728–5735. https://doi.org/10.1128/AEM.00308-310 (2010).
16. Jaswal, R. et al. Metagenomics-guided survey, isolation, and characterization of uranium-resistant microbiota from the Savannah River Site, USA. *Genes* **10**(5), 325. https://doi.org/10.3390/genes10050325 (2019).
17. Jaswal, R., Pathak, A. & Chauhan, A. Metagenomic evaluation of bacterial and fungal assemblages enriched within diffusion chambers and microbial traps containing uraniferous soils. *Microorganisms.* **7**(9), 324. https://doi.org/10.3390/microorganisms7090324 (2019).
18. Agarwal, M. et al. Proteogenomic analysis of *Burkholderia* species strains 25 and 46 isolated from uranium-rich soils reveals multiple mechanisms to cope with uranium stress. *Cells* **7**, 269. https://doi.org/10.3390/cells7120269 (2018).
19. Frossard, A., Hartmann, M. & Frey, B. Tolerance of the forest soil microbiome to increasing mercury concentrations. *Soil Biol. Biochem.* **105**, 162–176. https://doi.org/10.1016/j.soilbio.2016.11.016 (2017).
20. Amin, A. & Latif, Z. Isolation and characterization of H2S-producing yeast to detoxify mercury-containing compounds. *Int. Res. J. Microbiol.* **2**, 517–525 (2011).
21. Urík, M., Hlodák, M., Mikušová, P. & Matúš, P. Potential of microscopic fungi isolated from mercury contaminated soils to accumulate and volatilize mercury(II). *Water Air Soil Pollut.* **225**, 2219. https://doi.org/10.1007/s11270-014-2219-z (2014).
22. Abdelaziz, A.M., Hashem, A.H., Abd-Elsalam, K.A., Attia, M.S. Biodiversity of fungal endophytes. In: Abd-Elsalam, K.A., AbuQamar, S.F. (eds) Fungal endophytes Volume I. *Springer, Singapore*; https://doi.org/10.1007/978-981-97-7312-1_2 (2025).
23. Edwards, P. G. et al. Trophic dynamics of U, Ni, Hg, and other contaminants of potential concern on the Department of Energy's Savannah River Site. *Environ. Monit. Assess.* **186**, 481–500. https://doi.org/10.1007/s10661-013-3392-z (2014).
24. Campbell, K. R., Ford, C. J. & Levine, D. A. Mercury distribution in Poplar Creek, Oak Ridge, Tennessee, USA. *Environ. Toxicol. Chem.* **17**(7), 1191–1198. https://doi.org/10.1002/etc.5620170701 (1998).
25. Brooks, S. C. & Southworth, G. R. History of mercury use and environmental contamination at the Oak Ridge Y-12 Plant. *Environ Pollut.* **159**(1), 219–228. https://doi.org/10.1016/j.envpol.2010.09.009 (2011).
26. US Government Accountability Office (2024). Oak Ridge Mercury Cleanup: opportunities to enhance risk management and technology development. https://www.gao.gov/products/gao-24-107096
27. Seaman, J. C., Arey, J. S. & Bertsch, P. M. immobilization of nickel and other metals in contaminated sediments by hydroxyapatite addition. *J. Environment. Quality* **30**(2), 460–469. https://doi.org/10.2134/jeq2001.302460x (2001).
28. Harris, S., Xu, X. & Mills, G. Metal-sulfide dynamics in a constructed wetland in the Southeastern United States. *Wetlands Ecol. Manage* **28**, 847–861. https://doi.org/10.1007/s11273-020-09749-6 (2020).
29. Dahl, A. L., Sanseverino, J. & Gaillard, J. F. Bacterial bioreporter detects mercury in the presence of excess EDTA. *Environ. Chem.* **8**(6), 552. https://doi.org/10.1071/en11043 (2011).
30. Kabir, S., Rajendran, N., Amemiya, T. & Itoh, K. Quantitative measurement of fungal DNA extracted by three different methods using real-time polymerase chain reaction. *J. Biosci. Bioeng.* **96**(4), 337–343. https://doi.org/10.1016/s1389-1723(03)90133-2 (2003).
31. Fierer, N., Jackson, J. A., Vilgalys, R. & Jackson, R. B. Assessment of soil microbial community structure by use of taxon-specific quantitative PCR assays. *Appl. Environ. Microbiol.* **71**(7), 4117–4120. https://doi.org/10.1128/AEM.71.7.4117-4120.2005 (2005).
32. Parada, A. E., Needham, D. M. & Fuhrman, J. A. Every base matters: assessing small subunit rRNA primers for marine microbiomes with mock communities, time series, and global field samples. *Environ. Microbiol.* **18**, 1403–1414. https://doi.org/10.1111/1462-2920.13023 (2016).
33. White, T., Bruns, T., Lee, S. & Taylor, J. "Amplification and direct sequencing of fungal ribosomal RNA genes for phylogenetics," in PCR Protocols. A Guide to Methods and Applications, eds M. A. Innis, D. H. Gelfand, J. J. Sninsky, and T. J. White (San Diego, CA: Academic Press, 1990), 315–322.
34. Zhang, J., Kobert, K., Flouri, T. & Stamatakis, A. PEAR: a fast and accurate Illumina paired-end reAd merger. *Bioinformatics* **30**(5), 614–620. https://doi.org/10.1093/bioinformatics/btt593 (2014).
35. Tikhonov, M., Leach, R. W. & Wingreen, N. S. Interpreting 16S metagenomic data without clustering to achieve sub-OTU resolution. *ISME J.* **9**, 68–80. https://doi.org/10.1038/ismej.2014.117 (2015).

36. Edgar, R. C. Search and clustering orders of magnitude faster than BLAST. *Bioinformatics* **26**, 2460–2461. https://doi.org/10.1093/bioinformatics/btq461 (2010).
37. Nilsson, R. H. et al. Mycobiome diversity: high-throughput sequencing and identification of fungi. *Nat. Rev. Microbiol.* **17**(2), 95–109. https://doi.org/10.1038/s41579-018-0116-y (2019).
38. Douglas, G. M. et al. PICRUSt2: an improved and extensible approach for metagenome inference. *Nat. Biotechnol.* **38**(6), 685–688. https://doi.org/10.1038/s41587-020-0548-6 (2020).
39. Buchfink, B., Xie, C. & Huson, D. H. Fast and sensitive protein alignment using DIAMOND. *Nat. Methods* **12**(1), 59–60. https://doi.org/10.1038/nmeth.3176 (2015).
40. Huson, D. H., Auch, A. F., Qi, J. & Schuster, S. C. MEGAN analysis of metagenomic data. *Genome Res.* **17**(3), 377–386. https://doi.org/10.1101/gr.5969107 (2007).
41. Dhariwal, A. et al. MicrobiomeAnalyst: a web-based tool for comprehensive statistical, visual, and meta-analysis of microbiome data. *Nucleic Acids Res.* **45**, W180–W188. https://doi.org/10.1093/nar/gkx295 (2017).
42. Anderson, M. J. & Willis, T. J. Canonical analysis of principal coordinates: a useful method of constrained ordination for ecology. *Ecology* **84**, 511–525 (2003).
43. Lambertsson, L. & Nilsson, M. Organic material: the primary control on mercury methylation and ambient methyl mercury concentrations in estuarine sediments. *Environ. Sci. Technol.* **40**, 1822–1829. https://doi.org/10.1021/es051785h (2006).
44. Barkay, T., Gillman, M. W. & Turner, R. R. Effects of dissolved organic carbon and salinity on bioavailability of mercury. *Appl. Environment. Microbiol.* **63**, 4267–4271 (1997).
45. Fang, F., Wang, H. & Lin, Y. Spatial distribution, bioavailability, and health risk assessment of soil Hg in Wuhu urban area. *China. Environ Monit Assess.* **179**(1–4), 255–265. https://doi.org/10.1007/s10661-010-1733-8 (2011).
46. Różański, S. Ł, Castejón, J. M. P. & Fernández, G. G. Bioavailability and mobility of mercury in selected soil profiles. *Environ. Earth Sci.* **75**, 1065. https://doi.org/10.1007/s12665-016-5863-3 (2016).
47. Gorski, P. R., Armstrong, D. E., Hurley, J. P. & Krabbenhoft, D. P. Influence of natural dissolved organic carbon on the bioavailability of mercury to a freshwater alga. *Environ. Pollut.* **154**(1), 116–123. https://doi.org/10.1016/j.envpol.2007.12.004 (2008).
48. Lord, C. et al. Raccoon (Procyon lotor) as a bioindicator of mercury contamination at the US Department of Energy's Savannah River Site. *Arch. Environment. Contamin. Toxicol.* **43**, 356–363 (2002).
49. Liu, Y. R. Patterns of bacterial diversity along a long-term mercury-contaminated gradient in the paddy soils. *Microb Ecol* **68**, 575–583. https://doi.org/10.1007/s00248-014-0430-5 (2014).
50. Bott, T., Shaw, G. & Gregory, S. A simple method for testing and controlling inhibition in soil and sediment samples for qPCR. *J. Microbiol. Methods* https://doi.org/10.1016/j.mimet.2023.106795 (2023).
51. Durazzi, F. et al. Comparison between 16S rRNA and shotgun sequencing data for the taxonomic characterization of the gut microbiota. *Sci. Rep.* **11**, 3030. https://doi.org/10.1038/s41598-021-82726-y (2021).
52. Vetrovsky, T. & Baldrian, P. The variability of the 16S rRNA gene in bacterial genomes and its consequences for bacterial community analyses. *PLoS ONE* **8**(2), e57923. https://doi.org/10.1371/journal.pone.0057923 (2013).
53. Yue, Y., et al. Com-2seq: A compositional-aware method for differential abundance analysis of microbiome data. *bioRxiv*. https://doi.org/10.1101/2023.06.27.546795 (2023).
54. Pollock, J., Glendinning, L., Wisedchanwet, T. & Watson, M. The madness of microbiome: Attempting to find consensus "best practice" for 16S microbiome studies. *Appl. Environment. Microbiol.* **84**(7), e02627-e2717. https://doi.org/10.1128/AEM.02627-17 (2018).
55. Franzosa, E. A. et al. Identifying personal microbiomes using metagenomic codes. *Nat. Biotechnol.* **33**, 105–110. https://doi.org/10.1038/nbt.3125 (2015).
56. Yang, W. Components of rhizospheric bacterial communities of barley and their potential for plant growth promotion and biocontrol of Fusarium wilt of watermelon. *Braz J.* **50**(3), 749–757. https://doi.org/10.1007/s42770-019-00089-z (2019).
57. Nanjundappa, A., Ram, A., Ranadev, P., Revanna, A. & Bagyaraj, D. Pseudomonas species in soil as a natural resource for plant growth promotion and biocontrol characteristics-an overview. *Madras Agricult. J. 108* https://doi.org/10.29321/MAJ.10.000571 (2021).
58. Rani, A., Rockne, K. J., Drummond, J., Al-Hinai, M. & Ranjan, R. Geochemical influences and mercury methylation of a dental wastewater microbiome. *Sci. Rep.* **5**, 12872. https://doi.org/10.1038/srep12872 (2015).
59. Mahbub, K. R. et al. Mercury toxicity to Eisenia fetida in three different soils. *Environ. Sci. Pollut. Res.* **24**, 1261–1269. https://doi.org/10.1007/s11356-016-7869-5 (2017).
60. Wang, L. W. et al. Remediation of mercury-contaminated soil, water, and air: a review of emerging materials and innovative technologies. *Environ Int* **134**, 105281. https://doi.org/10.1016/j.envint.2019.105281 (2020).
61. Nakagawa, S. et al. Deep-sea vent epsilon-proteobacterial genomes provide insights into the emergence of pathogens. *Proc Natl. Acad Sci. USA* **104**, 12146–12150. https://doi.org/10.1073/pnas.0700687104 (2007).
62. Ivanova, E. P., Gorshkova, N. M. & Kurilenko, V. V. Tolerance of marine Proteobacteria of the genera Pseudoalteromonas and Alteromonas to heavy metals. *Microbiology* **70**, 239–241. https://doi.org/10.1023/A:1010498017807 (2001).
63. Garcia, Í. R. et al. Microbial resistance: the role of efflux pump superfamilies and their respective substrates. *Life Sci.* **295**, 120391. https://doi.org/10.1016/j.lfs.2022.120391 (2022).
64. Martinez, J. L. et al. Functional role of bacterial multidrug efflux pumps in microbial natural ecosystems. *FEMS Microbiol. Rev.* **33**(2), 430–449. https://doi.org/10.1111/j.1574-6976.2008.00157.x (2009).
65. Permina, E. A., Kazakov, A. E., Kalinina, O. V. & Gelfand, M. S. Comparative genomics of regulation of heavy metal resistance in Eubacteria. *BMC Microbiol.* **6**, 49. https://doi.org/10.1186/1471-2180-6-49 (2006).
66. Zhu, J. et al. Phylogenetic analysis of bacterial community composition in sediment contaminated with multiple heavy metals from the Xiangjiang River in China. *Mar. Pollut. Bull.* **70**(1–2), 134–139. https://doi.org/10.1016/j.marpolbul.2013.02.023 (2013).
67. Pathak, A. et al. Genome-centric evaluation of Burkholderia sp strain SRS-W-2–2016 resistant to high concentrations of uranium and nickel isolated from the Savannah River Site (SRS), USA. *Genomics Data* **12**, 62–68. https://doi.org/10.1016/j.gdata.2017.02.011 (2017).
68. Lin, H., Morrell-Falvey, J. L., Rao, B., Liang, L.,& Gu, B. (2014). Coupled Mercury–Cell Sorption, Reduction, and Oxidation on Methylmercury Production by Geobacter sulfurreducens PCA. United States: N. p.;https://doi.org/10.1021/es502537a
69. Kommu, N., Stothard, P., Chukwujindu, C., Pathak, A. & Chauhan, A. Utilizing a metagenome assembled genome approach revealed further insights into microbially mediated heavy-metal resistance in soils from a former nuclear materials production facility. *Appl. Microbiol.* **4**(1), 376–389. https://doi.org/10.3390/applmicrobiol401002 (2024).
70. Rudrik, J. T., Bawdon, R. E. & Guss, S. P. Determination of mercury and organomercurial resistance in obligate anaerobic bacteria. *Can J. Microbiol.* **31**(3), 276–281. https://doi.org/10.1139/m85-051 (1985).
71. Rasmussen, L. et al. Cultivation of hard-to-culture subsurface mercury-resistant bacteria and discovery of new merA gene sequences. *Appl. Environment. Microbiol.* **74**, 3795–3803. https://doi.org/10.1128/AEM.00049-08 (2008).
72. Tessler, M. et al. Large-scale differences in microbial biodiversity discovery between 16S amplicon and shotgun sequencing. *Sci. Rep.* **7**(1), 1–14. https://doi.org/10.1038/s41598-017-06665-3 (2017).
73. Laudadio, I. et al. Quantitative assessment of shotgun metagenomics and 16S rRNA amplicon sequencing in a human gut microbiome study. *OMICS* **22**(4), 248–254. https://doi.org/10.1089/omi.2018.0013 (2018).
74. Ruiz-Díez, B. et al. Mercury-resistant rhizobial bacteria isolated from nodules of leguminous plants growing in high Hg-contaminated soils. *Appl. Microbiol. Biotechnol.* **96**, 543–554. https://doi.org/10.1007/s00253-011-3832-z (2012).

75. Salmi, A. L. & Boulila, F. Heavy metals multi-tolerant Bradyrhizobium isolated from mercury mining region in Algeria. *J. Environment. Manag.* **289**, 112547. https://doi.org/10.1016/j.jenvman.2021.112547 (2021).
76. Nonnoi, F. et al. Metal tolerance of rhizobial strains isolated from nodules of herbaceous legumes (Medicago spp and Trifolium spp) growing in mercury-contaminated soils. *Appl. Soil Ecol.* **61**, 49–59. https://doi.org/10.1016/j.apsoil.2012.06.004 (2012).
77. Lu, X. et al. Anaerobic mercury methylation and demethylation by geobacter bemidjiensis bem. *Environment. Sci. Technol.* **50**(8), 4366–4373. https://doi.org/10.1021/acs.est.6b00401 (2016).
78. Koribanics, N. M. et al. Spatial distribution of a uranium-respiring betaproteobacterium at the Rifle CO field research site. *PLoS ONE* **10**, e0123378. https://doi.org/10.1371/journal.pone.0123378 (2015).
79. Rastelli, E., Buschi, E., Barone, G. & Beolchini, F. Fungi can be more effective than bacteria for the bioremediation of marine sediments highly contaminated with heavy metals. *Microorganisms* **10**(5), 993. https://doi.org/10.3390/microorganisms10050993 (2022).
80. Lin, Y., Ye, Y., Hu, Y. & Shi, H. The variation in microbial community structure under different heavy metal contamination levels in paddy soils. *Ecotoxicol. Environ. Saf.* **180**, 557–564 (2019).
81. Chauhan, A. et al. Physiological and comparative genomic analysis of Arthrobacter sp srs-w-1–2016 provides insights into niche adaptation for survival in uraniferous soils. *Genes (Basel)* **9**(1), 31. https://doi.org/10.3390/genes9010031 (2018).
82. Pan, R., Cao, L. & Zhang, R. Combined effects of Cu, Cd, Pb, and Zn on the growth and uptake of a consortium of Cu-resistant Penicillium sp. A1 and Cd-resistant Fusarium sp. A19. *J Hazard Mater* **171**(1–3), 761–766. https://doi.org/10.1016/j.jhazmat.2009.06.080 (2009).
83. Kurniati, E., Arfarita, N. & Imai, T. Potential use of Aspergillus flavus strain krp1 in using mercury contaminant. *Procedia Environment. Sci.* **20**, 254–260. https://doi.org/10.1016/j.proenv.2014.03.032 (2014).
84. Das, S. K., Das, A. R. & Guha, A. K. A study on the adsorption mechanism of mercury on Aspergillus versicolor biomass. *Environ. Sci. Technol.* **41**(24), 8281–8287. https://doi.org/10.1021/es070814g (2007).
85. Karunasagar, D., Arunachalam, J., Rashmi, K., Naveena, L. L. & Maruthi, M. P. Biosorption of inorganic and methyl mercury by a biosorbent from Aspergillus niger. *World J. Microbiol. Biotechnol.* **19**, 291–295. https://doi.org/10.1023/A:1023610425758 (2003).
86. North, N. N. et al. Change in bacterial community structure during in situ biostimulation of subsurface sediment cocontaminated with uranium and nitrate. *Appl. Environ. Microbiol.* **70**, 4911–4920. https://doi.org/10.1128/AEM.70.8.4911-4920.2004 (2004).
87. Schaefer, J. K. et al. Active transport, substrate specificity, and Hg(II) methylation in anaerobic bacteria. *Proc. Natl. Acad. Sci. U S A.* **108**(21), 8714–8719. https://doi.org/10.1073/pnas.1105781108 (2011).
88. Johnson, D. C., Dean, D. R., Smith, A. D. & Johnson, M. K. Structure, function, and formation of biological iron-sulfur clusters. *Annu. Rev. Biochem.* **74**, 247–281. https://doi.org/10.1146/annurev.biochem (2005).

Acknowledgement

This research was funded by the Department of Energy (DOE) Minority Serving Institution Partnership Program (MSIPP) task order agreement #800002172; the National Science Foundation award 2200615; Department of Energy's University Training & Research Program University Coal Research (UCR) and Historically Black Colleges and Universities and Other Minority Institutions (HBCU-OMI) award #DE-FE0032198; and the Department of Defense contract #W911NF2210145. Technical assistance provided by Drs. Meenakshi Agarwal and Rajesh S. Rathore are also appreciated. We also appreciate help provided by Dr. John Seaman from the Savannah River Ecology Laboratory (SREL) and Dr. Scott Brooks from the Oak Ridge National Lab (ORNL) for sample collection from the SRS and ORR ecosystems.

Author contributions

AC, AP, and RJ contributed to the conception and design of the study. AP, RJ, and AC organized the database and performed the statistical analysis. AP and AC wrote the first draft of the article. AC, CC, AP, and RJ wrote sections of the article. All authors contributed to the article revision and read and approved the submitted version. All authors have read and agreed to the published version of the manuscript.

Funding

This research was funded by the Department of Energy (DOE) Minority Serving Institution Partnership Program (MSIPP) task order agreement #800002172; the National Science Foundation award 2200615; Department of Energy's University Training & Research Program University Coal Research (UCR) and Historically Black Colleges and Universities and Other Minority Institutions (HBCU-OMI) award #DE-FE0032198; and the Department of Defense contract #W911NF2210145.

Declarations

Competing interests

The authors declare no competing interests.

Additional information

Supplementary Information The online version contains supplementary material available at https://doi.org/10.1038/s41598-025-25944-y.

Correspondence and requests for materials should be addressed to A.C.